Norcantharidin triggers cell death and DNA damage through S phase arrest and ROS-modulated apoptotic pathways in human urinary bladder carcinoma TSGH-8301 cells

Chien-Chih Yu[1], Fang-Yu Ko[2], Chun-Shu Yu[1], Jing-Pin Lin[3], Chin-Chung Lin[4], Yi-Ping Huang[5], Jai-Sing Yang[6] and Jing-Gung Chung[7,8*]

[1]School of Pharmacy, China Medical University, Taichung 404, Taiwan
[2]Department of Cosmeceutics, China Medical University, Taichung, Taiwan
[3]School of Chinese Medicine, China Medical University, Taichung, Taiwan
[4]Department of Chinese Medicine, Fong-Yuan Hospital, Department of Health, Executive Yuan, Taichung 420, Taiwan
[5]Department of Physiology, China Medical University, Taichung 404, Taiwan
[6]Department of Pharmacology, China Medical University, Taichung 404, Taiwan
[7]Department of Biological Science and Technology, China Medical University, Taichung 404, Taiwan
[8]Department of Biotechnology, Asia University, Taichung 413, Taiwan

Running title: norcantharidin induces ROS-mediated apoptosis in human bladder cancer cells

*Correspondence to: Jing-Gung Chung, Department of Biological Science and Technology, China Medical University, No 91, Hsueh-Shih Road, Taichung 40402, Taiwan. Tel: 886-4-22053366-2161, Fax: 886-4-2205 3764. E-mail: jgchung@mail.cmu.edu.tw

Abstract.

Norcantharidin (NTCD) is one of the ingredients of blister beetles which have been as Chinese medicine for long ago. The purpose of this study was to investigate the inhibitory effects of NTCD on TSGH8301 human bladder cancer cells in vitro and its anticancer mechanism. Cell morphological examination was photographed by phase-contrast microscope. The percentage of viable cells, cell cycle distribution, sub-G1 phase (apoptosis), reactive oxygen species production and the levels of mitochondrial membrane potential were conducted by flow cytometric assay. DNA condense and damage were performed by DAPI staining and Comet assay. Apoptosis associated protein expression in TSGH8301 cells after exposed to NTCD were examined, measured and determined by Western blotting and the protein translocation was conducted by confocal laser system microscope. Results indicated that NTCD induced cytotoxic effects including induced cell morphological changes and decreased the percentage of viability, induced S-phase arrest, sub-G1 phase (apoptosis) in TSGH8301 cells. The activities of caspase-3, -9 were up-regulated after NTCD treatment. Results from Western blotting indicated that NTCD up-regulated Fas, FasL, Bax, Bid, cytochrome c, caspase-3, -8 and -9 that led to induce apoptosis through Fas extrsinic patheway. Furthermore, NTCD induced AIF and Endo G that released from mitochondia then to induce apoptosis through mitochondria-independent pathway. NTCD also up-regulated ROS production and down-regulated $\Delta\Psi_m$ and ERK, JNK and p38 in TSGH8301 cells. These findings suggest that NTCD triggers apoptosis in TSGH8301 human bladder cancer cells via the Fas receptor, activation of the caspse-8, -9 and -3, mitochondrial-dependent and -independent pathways. NTCD may be useful for developing new therapeutic regimens for the treatment of bladder cancer.

Keywords: Norcantharidin; human bladder cancer TSGH 8301 cells; apoptosis; mitochondria

Introduction

In the worldwide, bladder cancer is one of the leading causes of death in human population. Bladder cancer is the fourth most common malignancy in men and the ninth most common in women in United States (1). In Taiwan, about 3.0 individuals per 100,000 die annually from bladder cancer based on the 2008 report from the Department of Health, R.O.C. (Taiwan). Currently, the treatments for bladder cancer are still unsatisified, therefore, numerous studies have been focused to find or synthesis the new compounds and to investigate the molecular mechanisms of action from bioactive compounds in order to develop the chemopreventive and/or therapeutic agents (2).

The one of the best way for anticancer agent to treat cancer is to induce apoptosis of cancer cells. The characteristic morphological and biochemical changes of apoptosis are mediated by a series of gene regulation and cell-signaling pathways. It is well documented that apoptosis (programmed cell death) including the extrinsic pathway (3, 4) which is triggered via specific ligands and surface receptors (D95/Fas, tumor necrosis factor (TNF) and death receptors (3-5), the intrinsic pathway which is induced via DNA damage, cellular distress, hypoxia and cytotoxic agents (4). And the endoplasmic reticulum (ER) stress pathway via the interaction between the mitochondria and ER (6).

Mylabris (Chinese blistering beetle).was usually used in medicine such as

Mylabris phalerata Pall. and *M. cichorii Linn* and it is still used as a folk medicine today (7). The active constituent of mylabris is cantharidin (8). Norcantharidin (NCTD) is the demethylated analog of cantharidin isolated from natural blister beetles (9). NCTD induced apoptosis in hepatoma cells (10), inhibited tumor cell growth, invasion, and metastasis in nude mice bearing human gallbladder carcinoma (11) and induced cytotoxicity in HepG2 cells by apoptosis, which is mediated through ROS generation and mitochondrial pathway (12). Furthermore, numerous studies have reported that NCTD inhibited angiogenesis and breast cancer cell-line metastases without significant renal or liver toxicity (9, 19, 13-17).

However, NCTD has inhibitory activities against human bladder cancer cells remains unclear. In this study, we investigated the in vitro effects of NCTD on the growth of human bladder cancer cell line TSGH8301. We investigated the molecular mechanisms of action of NCTD on reactive oxygen species production associated with the induction of apoptosis and its down-stream targets.

Materials and Methods

Chemicals and reagents

Norcantharidin, dimethyl sulfoxide (DMSO), potassium phosphates, propidium iodide (PI), Tris-HCl, trypan blue and ribonuclease-A, were obtained from Sigma Chemical Co. (St. Louis, MO, USA). RPMI-1640 medium with 1.5 mM L-glutamine + 10% fetal bovine serum, penicillin-streptomycin, and trypsin-EDTA were obtained from Gibco BRL (Grand Island, NY, USA). Norcantharidin was prepared in DMSO and stored as small aliquots at -20C.

Cell culture

The TSGH 8301 human bladder carcinoma cells were purchased from the Food Industry Research and Development Institute (Hsinchu, Taiwan). TSGH 8301 cells were maintained on 75 cm^2 tissue culture flasks with RPMI-1640 medium (Gibco BRL, Grand Island, NY, USA) with 10% fetal bovine serum (Gibco BRL, Grand Island, NY, USA) and 1.5 mM L-glutamine were adjusted to contain 1.5 μg/l sodium bicarbonate and 1% penicillin-streptomycin (100 Units/ml penicillin and 100 μg/ml streptomycin) and grown at 37°C under a humidified 5% CO_2 atmosphere (18).

Cell morphology, viability, cell cycle distribution and apoptosis assays

TSGH 8301 cells were seeded in a 12-well plate at a concentration of $5x10^5$ cells/well for overnight then were incubated with 0, 10, 20, 30, 40 and 50 μM of NTCD at 37°C, 5% CO_2 and 95% air for 24 and 48 h. Cells were examined and photographed under phase-contrast microscope at 200x for morphological changes. Then cells in each well were harvested and were stained with PI (5 μg/ml) then all samples were measured the total percentage of viable cells by flow cytometry (Becton-Dickinson, San Jose, CA, USA) as previously described (18, 19). For cell cycle distribution and sub-G1 (apoptosis) determination, isolated cells from each treatment were fixed gently by putting 70% ethanol in 4°C overnight and then re-suspended in PBS containing 40 μg/ml PI and 0.1 mg/ml RNase and 0.1% Triton X-100 in dark room for 30 min at 37°C then were analyzed with a flow cytometer equipped with an argon ion laser at 488 nm wavelength (18, 19). In order to confirm whether or not NTCD induced cell morphological changes and decreased the total percentage of viable TSGH8301 cells, cells were pretreated with NAC then were treated with NTCD then were examined cell morphological changes and toital viable cells as described above.

DNA damage was measured by DAPI staining and Comet assay

Approximately $5x10^4$ cells/ml of TSGH 8301 cells on 12 well plate were individually treated with 0, 10, 20, 30, 40 and 50 μM of NTCD for 24 h. For DAPI staining, cells in each treatment were stained with DAPI (4,6-diamidino-2-phenylindole dihydrochloride), then were examined and photographed using a fluorescence microscope as previously described (18-20). For Comet assay, cells from each treatment were harvested by centrifugation, isolated and examined for DNA damage by using the Comet assay as previously described (18-20).

Detections of ROS (reactive oxygen species), mitochondrial membrane potential ($\Delta\Psi_m$) and caspase-3 activity in TSGH8301 cells

Approximately $5x10^4$ cells/ml of TSGH 8301 cells were placed in 12-well plate for 24 h then were individually treated with 30 μM of NTCD for 0, 12, 24, 48 and 72 h then cells from each treatment were harvested by centrifugation and re-suspended in 500 μl of 2,7-Dichlorodihydrofluorescein diacetate (DCFH-DA) (10 μM) for ROS, in 500 μl of $DiOC_6$ (4 μmol/L) for $\Delta\Psi_m$ and in ul ----- for caspase-3 activity determinations as described previously (18, 19). Cells from each treatment were incubated at 37°C for 30 min before being analyzed by flow cytometry as described previously (18-19). Or cells in each treatment were pretreated with NAC then were treated with NTCD for 24 h then were harvested for measuring the ROS and NAO productions, the levels of$\Delta\Psi_m$ and catalase expression.

Determination of cell cycle and apoptosis associated proteins by Western blotting

Approximately $5x10^6$ cells of TSGH 8301 cells were maintained in 6-well plate then were treated with 30 μM NTCD for 0, 6, 12, 24, 48 and 72 h. Cells from each

treatment were harvested in tube with lysis buffer containing 40mM Tris–HCl (pH 7.4), 10mM EDTA, 120mM NaCl, 1mM dithiothreitol, 0.1% Nonide P-40 and the total proteins were quantitated as described previously (18-20). The total proteins (30 μg) from each treatment were individually loaded into the gel for Western blot analysis and all samples were performed using 10% Tris-glycine-SDS-polyacrylamide gels for 30 min then the proteins were transferred to a nitrocellulose membrane by electroblotting (18-20). Then the transferred membrane were incubated with primary antibodies such as (A) p27, p21 and p53 (Santa Cruz Biotechnology, CA); (B) caspase—8, -9 and -3; (C) Bax and Bid; (D) AIF, Endo G and cytochrome c; (E) Fas and FasL; (F) p-ERK, JNK and p-p38 (R&D Systems, Minneapolis, USA) then were washed followed by incubated secondary antibody for enhanced chemiluminescence (NEN Life Science Products, Inc, Boston, MA, USA) as described previously (18-20). Anti-b-tubulin (a mouse monoclonal antibody) was used as a loading control.

Confocal laser scanning microscopy to show protein translocation in TSGH8301 cells

TSGH 8301 cells (5×10^4 cells/well) were cultured on 4-well chamber slides then were treated without or with 30 μM NTCD for 24 h, cells on the slides were fixed in 4% formaldehyde in PBS for 15 min, permeabilized with 0.3% Triton-X 100 in PBS for 1 h with blocking of non-specific binding sites using 2% BSA as described previously (20). Primary antibodies to AIF and Endo G (1:100 dilution) (green fluorescence) were used to stain the fixed cells for overnight then were washed twice with PBS and were stained with secondary antibody (FITC-conjugated goat anti-mouse IgG at 1:100 dilution), and followed by DNA staining with mitotracker (red fluorescence) as described previously (20). All samples were photomicrographed and were obtained

using a Leica TCS SP2 Confocal Spectral Microscope (20).

Statistical analysis.

The results in this study are showing in mean±SD and the difference between the NTCD-treated and control groups were analyzed by Student's *t*-test, a probability of $p<0.05$ being considered significant.

Results

Effects of NTCD on cell morphology, viability, cell cycle distribution and sub-G1 phase in TSGH8301 cells

The effects of the growth inhibition of NTCD on TSGH8301 cells were examined the morphological changes under phase-contrast microscope, viability, cell cycle distribution and sub-G1 (apoptosis) by using flow cytometric assay and the results are showing in Figure 1A, B and C and Figure 2A and B. Increasing the concentrations of NTCD and/or time of incubation led to increase morphological changes (Fig. 1A and B) and decrease the percentage of viability (Fig. 1C). The 30 μM NTCD significantly decreased by almost 48 % the viable cells at 48 h treatment. Figure 2A and B showed that TSGH 8301 cells after were exposed to 30 μM of NTCD for various time incubation increased the percentage of cells in S phase by time-dependent. That the sub-G1 groups (apoptosis) also appeared in the cell cycle distribution and these effects are time-dependent responses.

Effects of NTCD on DNA damage in TSGH 8301 cells

The effects of NTCD on DNA damage of TSGH8301 cells were examined by Comet assay and DAPI staining. The TSGH 3801 cells were treated with various

concentrations of NTCD for 24 h then were isolated for DAPI staining and comet assay. The results are presented in Figure 3A and B, which indicated that NTCD induced DNA condensation and decreased the cell number (Fig. 3A) and induced DNAS damage (Fig. 3B) and those effects are in a dose-dependent manner.

Effects of NTCD on the levels of reactive oxygen species (ROS) and mitochondrial membrane potential ($\Delta\Psi_m$) and caspase-3 activity in TSGH 8301 cells

In order to examine whether or not NTCD-induced apoptosis via contributions from the ROS production, mitochondrial and caspase-3 pathway, TSGH 8301 cells were treated with 30 μM NTCD for the various time periods, the levels in ROS productions $\Delta\Psi m$ and caspase-3 activity were measured and determined by flow cytometric assay and the results are present in Figure 4A, B and C. Figure3 indicated NTCD increase the productions of ROS (Fig. 4A) and decreased the levels of $\Delta\Psi m$ (Fig. 4B) after compared with the control group. The figure 4C also showed that NTCD induced the activity of caspase-3 in TSGH8301 cells. These effects are time-dependent responses.

NAC pretreatment affect NTCD induced morphological changes, viability, reactive oxygen species (ROS) productions, the levels of mitochondrial membrane potential ($\Delta\Psi m$) and NAO and catalase productions in TSGH 8301 cells.

To confirm the role of ROS in NTCD induced cell death in TSGH8301 cells, cells were pretreated with ROS scavenger (N-------) then were treated with 30 UM NTCD for 24 h then cells were examined the cell morphological changes (Fig. 5A), total percentage of viable cells (Fig. 5B), ROS production (Fig. 5C), the levels of$\Delta\Psi m$ (Fig. 5D), NAO production (Fig. 5E). Figure 5 indicated that after cells were pretreated with NAC then decreased the cell morphological changes (Fig. 5A) and

increase the viable cell number (Fig. 5B), decreased the ROS production (Fig. 5C) and increased the levels of $\Delta\Psi m$ (Fig. 5D) but did not significant affects the NAO production in TSGH8301 cells. Figure 5F indicated TSGH8301 cells after treated with NTCD led to increase the catalase expression which is a time –responses.

Effects of NTCD on the associated proteins levels of apoptosis in TSGH 8301 cells

In order to investigate NTCD-induced apoptosis may through the possible signaling pathways in TSGH 8301 cells, cells were treated with 30μM of NTCD for various time periods then the protein levels were analyzed by Western blotting and results are shown in Figure 6, where NTCD increased p27, p21 and p53 (Fig. 6A), caspase-8, -9, -3 (Fig. 6B), Bax and Bid (fig. 6C), AIF, Endo G and cytochrome c (Fig. 6D), Fas and FasL (Fig. 6E) and p-ERK and p-p38 (Fig. 6F) but decreased the levels of JNK (Fig. 6F) in TSGH 8301 cells, that were led to apoptosis. Thus, we suggest that NTCD-induced apoptosis is mediated by the mitochondrial and ROS induced ER stress pathways.

Effects of NTCD on the apoptotic associated protein translocation in TSGH 8301 cells

In order to confirm NTCD affected apoptotic associated protein translocation in TSGH 8301 cells, 5×10^4 cells/well cells were plated on 4-well chamber slides then were treated with 30 μM NTCD for 24 h and then were stained by primary antibody and secondary antibody, were examined and photographed by confocal laser microscopic systems. The results are present in Figure 7A and B, due to the photographs have demonstrated that after merged in Figure 7A which indicated that Endo G (Fig. 7A) and AIF (Fig. 7B) are released from mitochondria then translocated to nuclei because the nuclei colors already change to orange that mean protein have

migrated to nuclei. Furthermore, based on the double immunofluorescence labelling it was clearly confirmed by means of confocal scanning microscopy indicated that the Endo G and AIF were increased after exposed to NTCD in TSGH 8301 cells

Discussion

In the present study, results from several observations have demonstrated that NTCD induced apoptosis in bladder cancer TSGH8301 cells and its possible associated mechanism. The TSGH8301 cells treated with NTCD displayed PI - or DAPI-stained condensed nuclei and a sub-G1 DNA phase of PI-stained nuclei analyzed by flow cytometry. Figure 2 indicated that he number of S-phase cells increased when the number of apoptotic cells increased, as a result of treatment with NTCD. However, there was an apparent decrease in the number of G0/G1 and G2/M phase cells within 72 h. Increase the NTCD treated time, the number of G0/G1 and G2/M phase cells gradually decreased and increase the Sub-G1 cells (Fig. 2A and B). This is not agreement with other reports demonstrated that NTCD may cause rapid apoptosis in S-phase cells and delayed apoptosis in G2/M arrested cells of colorectal cancer cells (8) that me b edue to the differences of cancer cells.

In this study, results showed that 1) NTCD decreased viable cells and induced S-phase arrest (Fig. 2). Figure 6A also showed that NTCD increased the levels of p53, p27 and p21 that may led to S phase arrest. NTCD induced apoptosis based on DAPI-staining and Sub-G1 phase in cell cycle analys of TSGH8301 cells. Flow cytometric assay also showed NTCD promoted caspase-3 activation (Fig. 4C) that was also confirm in Western blttting results (Figure 6B) demonstratedthen NTCD promoted activeve form of caspase-8, -3 and caspase-9 (Fig. 6B). It is well documentd that apoptosis can be divided into caspase- dependent and –independent signal

pathway (22, 23). Thus, herein, NTCD induced apoptosis in TSGH8301 cells was via caspase-dependent pathway. It was reported that Fas and FAS ligand activation involved in drug-induced apoptosis in solid cancer and leukemia cell lines (24). Our results from Western blotting (Fig. 6C) indicated that NTCD promoted Fas and FasL in TSGH8301 cells. NTCD induced apoptosis may through the Fas and FasL pathway. This is in agreement with other reports demonstrated that NTCD-treated cells showed the activation of caspase 8 which has been found to be a prominent signaling caspase involved in initiation of apoptosis by CD95 (8, 25, 26).

Flow cytometric assay also showed that NTCD promoted the ROS production and decreased the levels of $\Delta\Psi m$ (Fig. 4A and B). This is in agreement with other report indicated that NCTD induced cytotoxicity in human liver cancer HepG2 cells by apoptosis, which is mediated through ROS generation and mitochondrial pathway (27). It was reported that agents decreased the levels of $\Delta\Psi m$ which may led to apoptosis in cancer cells through the mitochondria-dependent pathway (28) which are involved in AIF, Endo G release from mitochondria for led to apoptosis via caspase-independent pathway (29). Herein, our results also showed that NTCD promoted the expression of AIF and Endo G (Fig. 6D) and they also confirm by confocal laser system microscope (Fig. 7A and B). These findings are the novel finding and may suggest that NTCD induced apoptosis in TSGH8301 cells may via caspase-dependent, -independent and mitochondrial-dependent pathways. Our results also showed that NTCD promoted Bax and BID levels (Fog. 6E). Numerous studies have been shown that some Bax, Bcl-XL, Mcl-1, Bcl-2, and Bid are located on the mitochondrial membrane, they can alter the permeability of the mitochondrial membrane for causing the activations of caspases then led to apoptosis (30-32). This is in agreement with other report show that NCTD inhibited the in vitro and ex vivo growth of human lung cancer A549 cells and regulated the expressions of Bcl-2 and

Bax proteins in a dose-dependent manner (33).

Our results from Figure 4A also showed that NTCD promoted the productions of ROS in TSGH 8301 cells. Furthermore, we also pretreated cells with NAC then followed by NTCD led to NCTD -induced increase inROS can be abolished or attenuated by NAC (antioxidant). This is in agreement with other reports indicated that the NCTD -induced increase in ROS and antiproliferation of human liver cancer HepG2 cells are apparently dependent on ROS generation (33). Thus, in the present studies, our results demonstrated that NTCD promoted ROS production and decreased the levels of$\Delta\Psi m$ then led to apoptosis. Other reports have been shown that in cancer cells after exposed to antcancer agent which led to the generation of ROS may contribute to mitochondrial damage and lead to cell death by acting as an apoptotic signaling molecule (34, 35). Furthermore, in the present study, ERK, JNK, and p38 were all found to be activated in TSGH 8301 cells after exposed to NTCD. Thus, NTCd induced cytotoxicity could be due to the induced JNK activation in nTSGH8301 cells.

In conclusion, based on these results, we can summarized these findings regarding NTCD efficiently inhibits the growth of TSGH8301 human bladder cancer cells via, Fas receptor led to caspase-3 activation for apoptosis named mitochondria-independent pathways and other pathway through mitochondria-dependent signal pathways led to release of AIF and Endo G then cause apoptosis. Overall, the possible signal pathways of NTCd induced apoptosis in TSGH8301 cells is showing in Figure 8. Further investigation on both *in vivo* and *in vitro* bladder cancer models is needed.

Acknowledgement

References

1. Chen RJ, Ho CT, Wang YJ. Pterostilbene induces autophagy and apoptosis in sensitive and chemoresistant human bladder cancer cells. Mol. Nutr. Food Res. 2010, 54, 1-14.

2. Singh RP, Dhanalakshmi S, Agarwal R. 2002. Phytochemicals as cell cycle modulators--a less toxic approach in halting human cancers, Cell Cycle 1:156-161

3. Degterev A, Boyce M, Yuan J. 2003. A decade of caspases. Oncogene 22:8543-8567.

4. Ziegler DS, Kung AL. 2008. Therapeutic targeting of apoptosis pathways in cancer. Current opinion in oncology 20:97-103.

5. Klein S, McCormick F, Levitzki A. 2005. Killing time for cancer cells. Nature reviews 5:573-580.

6. Gamet-Payrastre L, Li P, Lumeau S, Cassar G, Dupont MA, Chevolleau S, Gasc N, Tulliez J, Terce F. Sulforaphane, a naturally occurring isothiocyanate, induces cell cycle arrest and apoptosis in HT29 human colon cancer cells. Cancer Research 60, 1426-1433, 2000.

7. Wang GS (1989) Medical uses of mylabris in ancient China and recent studies. J Ethnopharmacol 26:147–162

8. F. Peng A Y.-Q. Wei A L. Tian A L. Yang A X. Zhao Y. Lu A Y.-Q. Mao A B. Kan A S. Lei A G.-S. Wang Y. Jiang A Q.-R. Wang A F. Luo A L.-Q. Zou A J.-Y. Liu. Induction of apoptosis by norcantharidin in human colorectal carcinoma cell lines: involvement of the CD95 receptor/ ligand. J Cancer Res Clin Oncol (2002) 128: 223-230

9. HuangY, Liu Q, Liu K, Yagasaki K and Zhang G. 2009. Suppression of growth of highly-metastatic human breast cancer cells by norcantharidin and its

mechanisms of action. Cytotechnology (2009) 59:201–208

10. Chen YN, Chen JC, Yin SC, Wang GS, Tsauer W, Hsu SF, Hsu SL (2002) Effector mechanisms of norcantharidininduced mitotic arrest and apoptosis in human hepatoma cells. Int J Cancer 100:158–165
11. Fan YZ, Zhao ZM, Fu JY, Chen CQ (2006) Anti-tumor mechanism of norcantharidin for the implanted tumors of human gallbladder carcinoma in nude mice in vivo. Zhonghua Wai Ke Za Zhi 44:618–622
12. Chang C, Zhu yQ, Mei JJ, Liu SG, Luo J. 2010. Involvement of mitochondrial pathway in NCTD-induced cytotoxicity in human hepG2 cells
13. Luan J, Duan H, Liu Q, Yagasaki K, Zhang G (2010) Inhibitory effects of norcantharidin against human lung cancer cell growth and migration. Cytotechnology 62(4):349–355
14. Chen YJ, Tsai YM, Kuo CD, Ku KL, Shie HS, Liao HF (2009) Norcantharidin is a small-molecule synthetic compound with anti-angiogenesis effect. Life Sci 85(17–18):642–651
15. Kok SH, Cheng SJ, Hong CY, Lee JJ, Lin SK, Kuo YS, Chiang CP, Kuo MY (2005) Norcantharidin-induced apoptosis in oral cancer cells is associated with an increase of proapoptotic to antiapoptotic protein ratio. Cancer Lett 217(1):43–52
16. Kok SH, Hong CY, Kuo MY, Lee CH, Lee JJ, Lou IU, Lee MS, Hsiao M, Lin SK (2003) Comparisons of norcantharidin cytotoxic effects on oral cancer cells and normal buccal keratinocytes. Oral Oncol 39(1):19–26
17. Peng C, Liu X, Liu E, Xu K, Niu W, Chen R, Wang J, Zhang Z, Lin P, Wang J, Agrez M, Niu J (2009) Norcantharidin induces HT-29 colon cancer cell apoptosis through the alphavbeta6-extracellular signal-related kinase signaling pathway. Cancer Sci 100(12):2302–2308.

18. Hsu SC, Yu CC, Yang JS, Lai KC, Wu SH, Lin JJ, Kuo JH, Yang ST, Huang CC, Kuo SC, Chung JG. A novel synthetic 2-(3-methoxyphenyl)-6,7-methylenedioxoquinolin-4-one arrests the G2/M phase arrest via Cdc25c and induces apoptosis through caspase- and mitochondria-dependent pathways in TSGH8301 human bladder cancer cells. Int J Oncol. 2012 Mar;40(3):731-8.

19. Lin ML, Lu YC, Chung JG, Li YC, Wang SG, N G SH, Wu CY, Su HL, Chen SS. Aloe-emodin induces apoptosis of human nasopharyngeal carcinoma cells via caspase-8-mediated activation of the mitochondrial death pathway. Cancer Lett. 2010 May 1;291(1):46-58.

20. Kuo JH, Chu YL, Yang JS, Lin JP, Lai KC, Kuo HM, Hsia TC, Chung JG. Cantharidin induces apoptosis in human bladder cancer TSGH 8301 cells through mitochondria-dependent signal pathways. Int J Oncol. 2010 Nov;37(5):1243-50.

21.

22.

23.

24. Mu··ller M, Strand S, Hug H, Heinemann EM, Walczak H, Hofmann WJ, Stremmel W, Krammer PH, Galle PR (1997) Druginduced apoptosis in hepatoma cells is mediated by the CD95 (APO-1/Fas) receptor/ligand system and involves activation of wild-type p53. J Clin Invest 99:403–413

25. Boldin MP, Goncharov TM, Goltsev YV, Wallach D (1996) Involvement of MACH, a novel MORT/FADD-interacting protease in Fas/APO-1- and TNF receptor-induced cell death. Cell 85:803–815

26. Glick RD, Swendeman SL, Coffey DC, Rifkind RA, Marks PA, Richon VM, Quaglia PL (1999) Hybrid polar histone deacetylase inhibitor induces apoptosis

and CD95/CD95 ligand expression in human neuroblastoma. Cancer Res 59:4392–4399

27. Chang C, Zhu YQ, Mei JJ , Liu SQ , Luo J. 2010. Involvement of mitochondrial pathway in NCTD-induced cytotoxicity in human hepG2 cells. Journal of Experimental & Clinical Cancer Research 2010, 29:145-153

28.

29.

30. Huan SK, Lee HH, Liu DZ, Wu CC, Wang CC. Cantharidin-induced cytotoxicity and cyclooxygenase 2 expression in human bladder carcinoma cell line. Toxicology 2006; 223: 136-43.

31. Rauh R, Kahl S, Boechzelt H, Bauer R, Kaina B, Efferth T. Molecular biology of cantharidin in cancer cells. Chin Med 2007; 2: 8.

32. Adams JM, Cory S. The Bcl-2 protein family: arbiters of cell survival. Science 281, 322-1326, 1998.

33. Luan J, Duan H, Liu Q, Yagasaki K, Zhang G. 2010. Inhibitory effects of norcantharidin against human lung cancer cell growth and migration. Cytotechnology (2010) 62:349–355

34. Zhang R, Humphreys I, Sahu RP, Shi Y, Srivastava SK: In vitro and in vivo induction of apoptosis by capsaicin in pancreatic cancer cells is mediated through ROS generation and mitochondrial death pathway. Apoptosis 2008, , 13: 1465-1478.

35. Ott M, Gogvadze V, Orrenius S, Zhivotovsky B: Mitochondria, oxidative stress and cell death. Apoptosis 2007, 12:913-22.

Figure legends

Figure 1. norantharidin (NTCD) induced morphological changes and affected the viability of TSGH 8301 human bladder cancer cells. Cells in 12-well plate were treated with 0, 10, 20, 30, 40 and 50 μM of NCTD for 24 and 48 h then cells were examined and photographed for morphological changes (A and B) by phase-contrast microscope. And cells were harvested for determination of viability (C) by using flow cytometeric assay as described in Materials and Methods. Significantly different from the 0 h treatment (control group) at *p<0.05.

Figure 2. NTCD induced cell cycle arrest and sub-G1 in TSGH 8301 cells. Cells were treated with 0 and 30 μM of NTCD for 0, 6, 12, 24, 48 and 72 h then cells were harvested for examinations of cell cycle distribution by flow cytometer as described in Materials and Methods. A: representative profiles; B: percentage of cell distribution. Significantly different from the 0 h treatment (control group) at *p<0.05.

Figure 3. NTCD induced DNA damage in TSGH 8301 cells. Cells were treated with 0, 10, 20, 30, 40 and 50 μM of NTCD for 24 h then cells from each well were harvested for examinations of DNA damage by DAPI staining (A) or Comet assay (B) as described in materials and methods. Significantly different from the 0 h treatment (control group) at *p<0.05.

Figure 4. NTCD induced reactive oxygen species (ROS) productions and decreased the levels of mitochondrial membrane potential ($\Delta\Psi m$) and induced caspase-3 activation in TSGH 8301 cells. TSGH 8301 cells ($5x10^5$ cells/ml) were treated with 30 μM of NTCD for different time periods. Cells were harvested for the percentage of ROS (A), $\Delta\Psi m$ (B) and caspase- activity (C) that were stained by DCFH-DA, Indo-1/AM and --------, respectively. The stained cells were determined by flow cytometry as described in the Materials and Methods. Values are means±SD (n=3). Significantly different from the 0 h treatment (control group) at *p<0.05.

Figure 5. NAC pretreatment affect NTCD induced morphological changes, viability , reactive oxygen species (ROS) productions, the levels of mitochondrial membrane

potential ($\Delta\Psi m$) and NAO and catalase productions in TSGH 8301 cells. TSGH 8301 cells ($5x10^5$ cells/ml) were pretreated with NAC then were treated with 30 μM of NTCD for different time periods. Cells were examined and photographed for morphological changes examination (A) then were harvested for the percentage of Viavle cells (B) and ROS production (C), levels of $\Delta\Psi m$ (D), NAO production (E). The stained cells were determined by flow cytometry as described in the Materials and Methods. Or cells were examined catalase expression (F) by Western blotting. Values are means±SD (n=3). Significantly different from the 0 h treatment (control group) at $*p<0.05$.

Figure 6. NTCD affects the proteins levels of G0/G1 arrest and apoptosis in TSGH 8301 cells. Cells were treated with 30 μM of NTCD for 0, 6, 12, 24, 48 and 72 h then the total proteins were prepared and detected by Western blotting as described in Materials and Methods. Respectively, primary antibodies for (A) p27, p21 and p53; (B) caspase-8, -9 and -3; (C) bax and Bid; (D) AIF, Endo G and cytochrome c; (E) Fas and FasL; (F)p-pERK, JNK and p-p38 were examined by Western blotting as described in Materials and Methods. .

Figure 7. NTCD affected Endo G and AIF distribution in TSGH 8301 cells. Cells were incubated with 30 μM NTCD for 24 h then were fixed and stained with primary antibodies to Endo G (A) and AIF (B) before FITC-labeled secondary antibodies were used (green fluorescence) and the proteins were detected by a confocal laser microscopic system as described in Materials and methods. The nuclei were stained by mitotracker (red fluorescence). Areas of colocalization between AIF and Endo G expressions and cytoplasm and nuclei in the merged panels are yellow. Scale bar, 40 μm.

Figure 8. The proposed model of molecular signal pathways from TSGH 9301 cells

after exposed to norcantharidin.

Figure 1

A

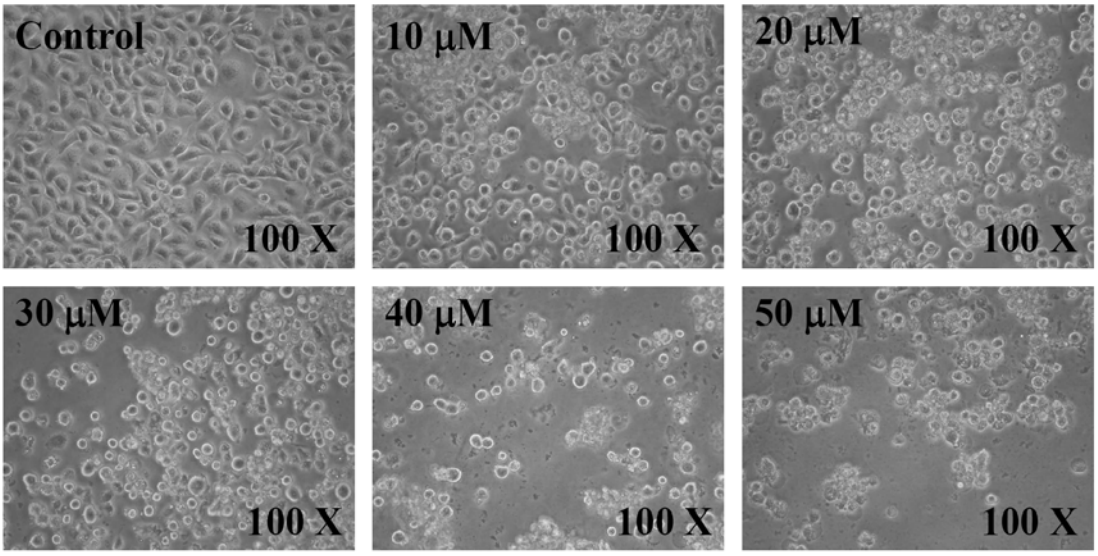

B

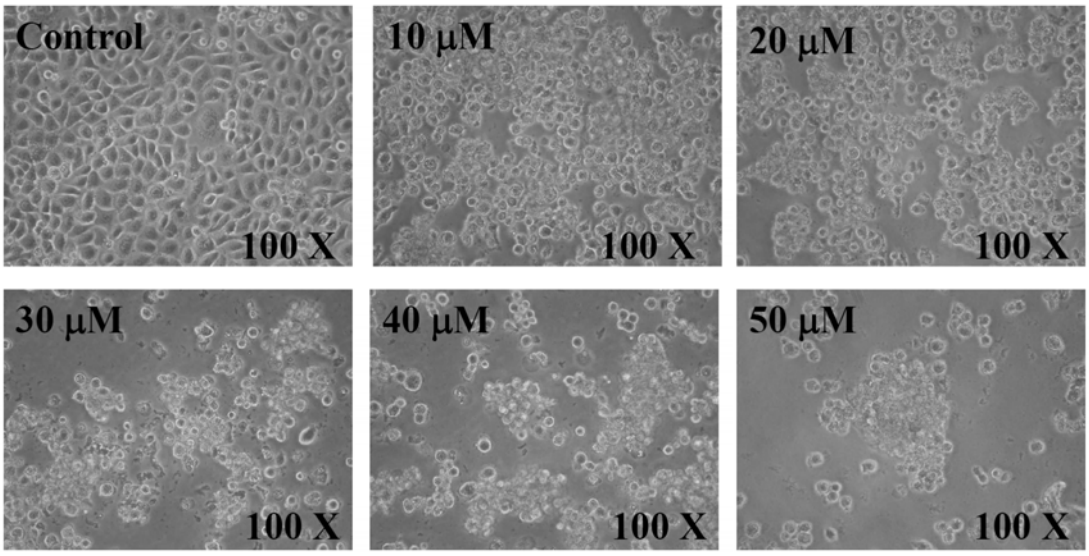

C

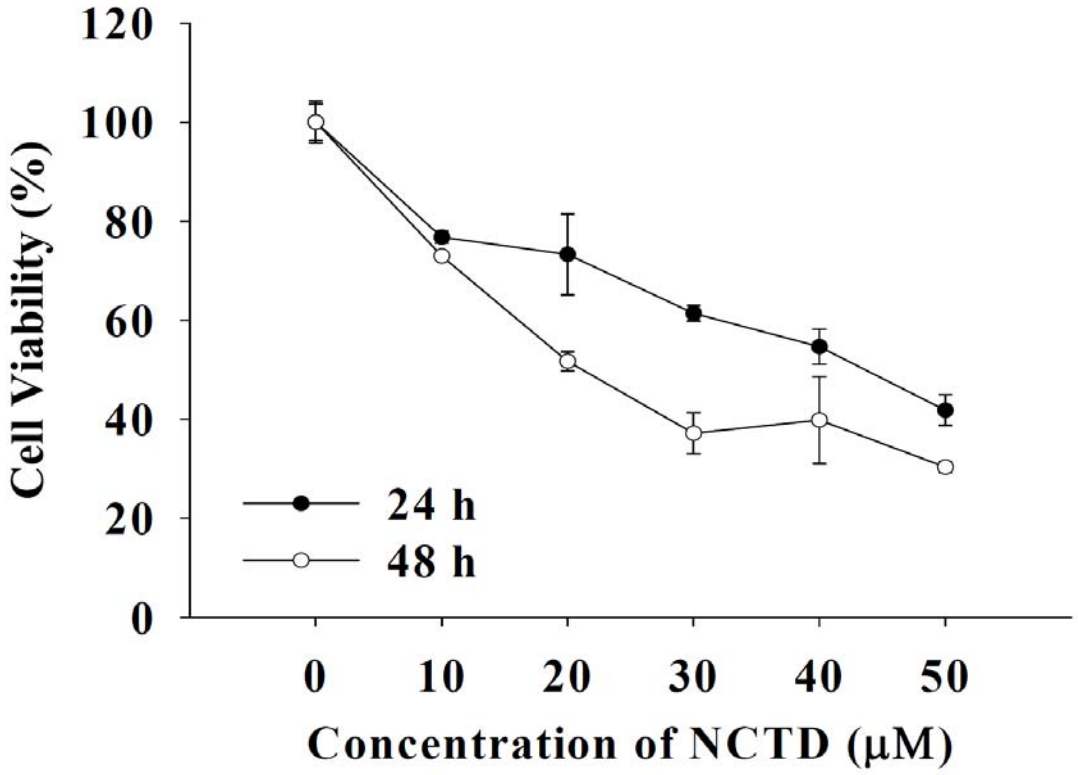
120
100
80
60
40
20
0
Cell Viability (%)
24 h
48 h
0
10
20
30
40
50
Concentration of NCTD (μM)

Figure 2

A

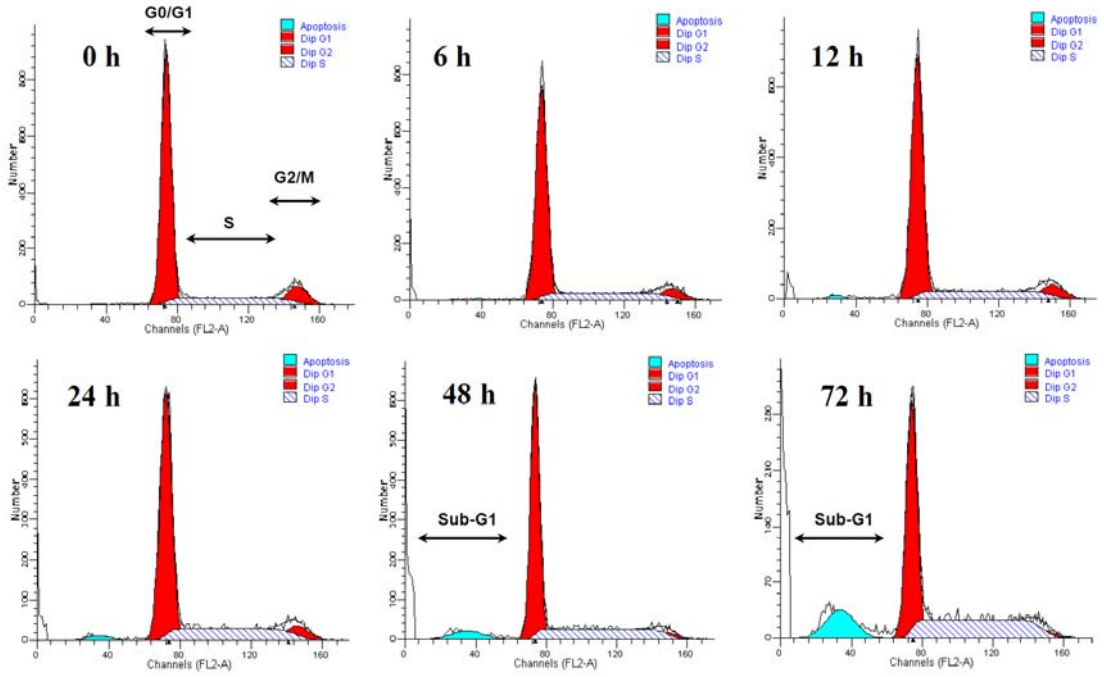
0 h
G0/G1
S
G2/M
6 h
12 h
24 h
48 h
Sub-G1
72 h
Sub-G1
Apoptosis
Dip G1
Dip G2
Dip S
Number
Channels (FL2-A)

B

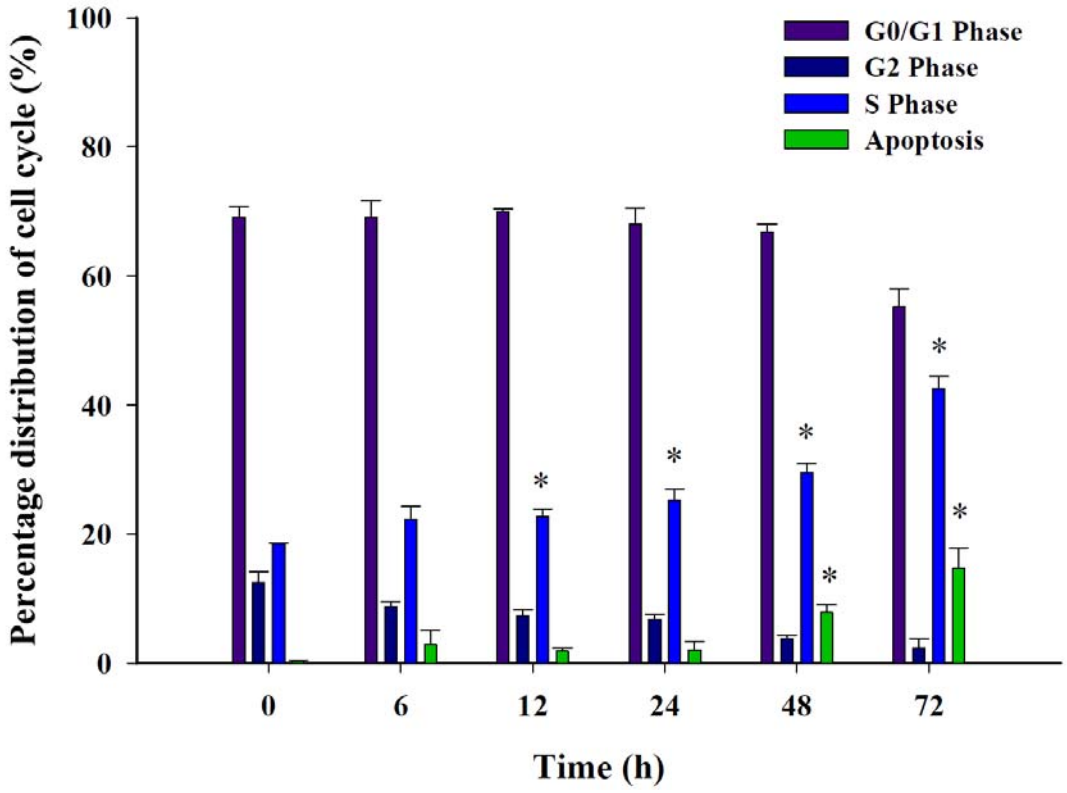
G0/G1 Phase
G2 Phase
S Phase
Apoptosis
Percentage distribution of cell cycle (%)
100
80
60
40
20
0
0
6
12
24
48
72
Time (h)
*

Figure 3

A

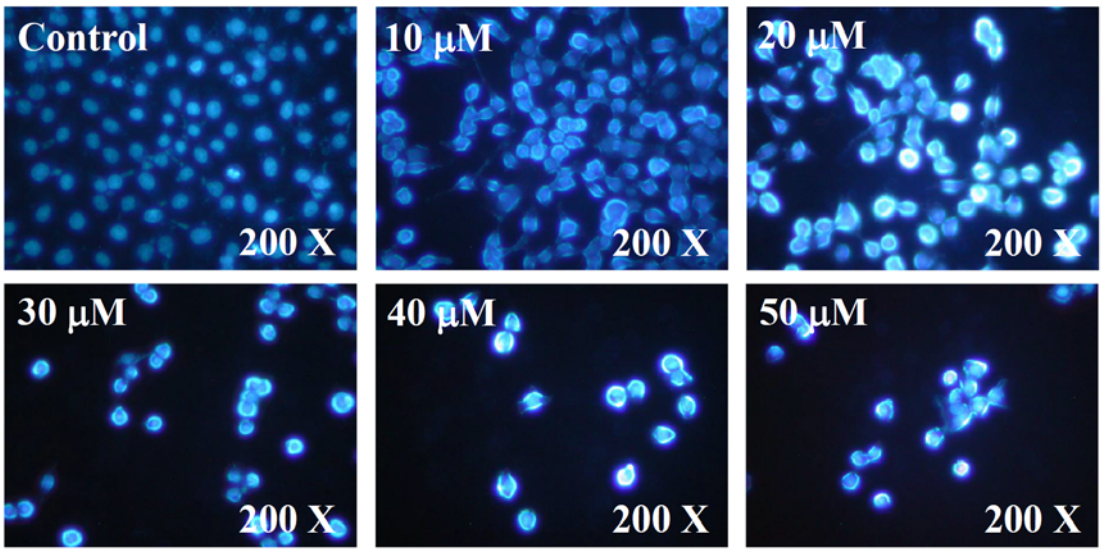
Control
200 X
10 μM
200 X
20 μM
200 X
30 μM
200 X
40 μM
200 X
50 μM
200 X

B

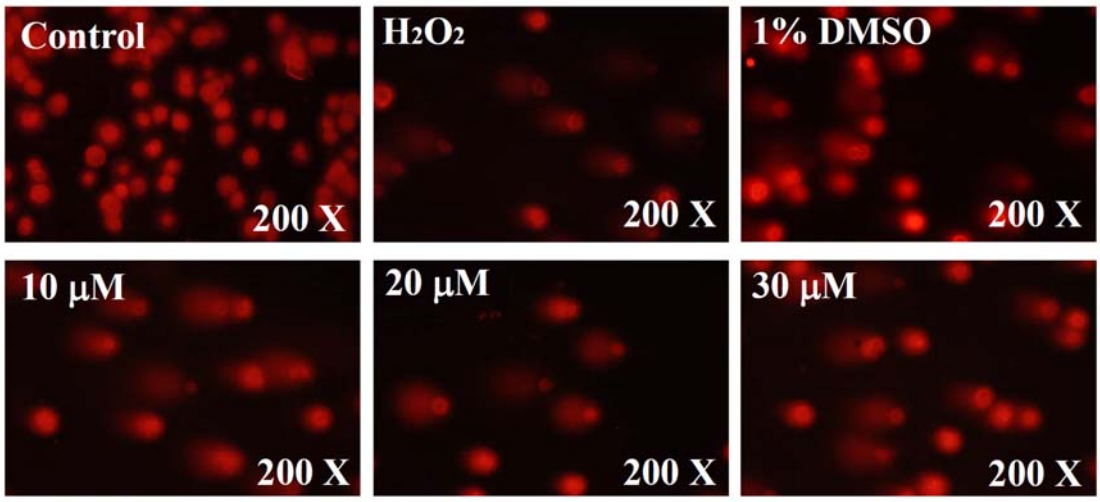
Control
200 X
H2O2
200 X
1% DMSO
200 X
10 μM
200 X
20 μM
200 X
30 μM
200 X

Figure 4

A

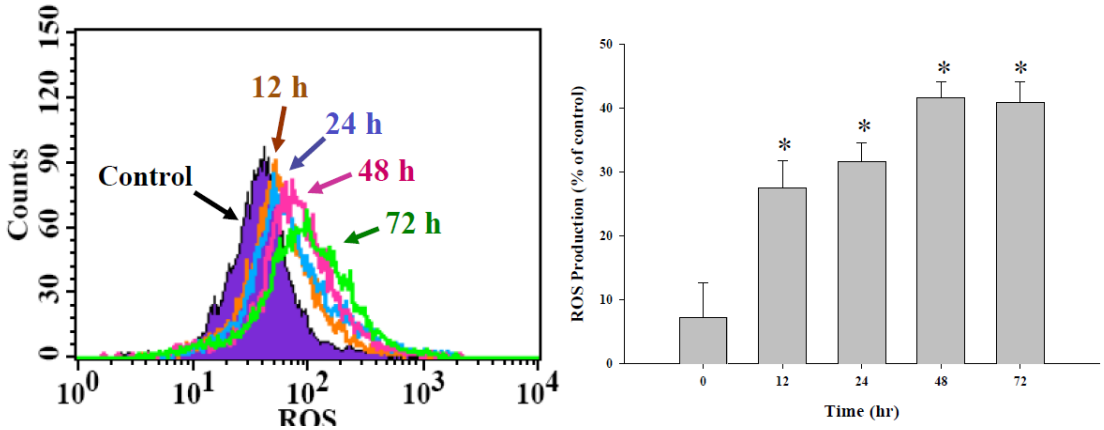
Counts
ROS
Control
12 h
24 h
48 h
72 h
ROS Production (% of control)
Time (hr)

B

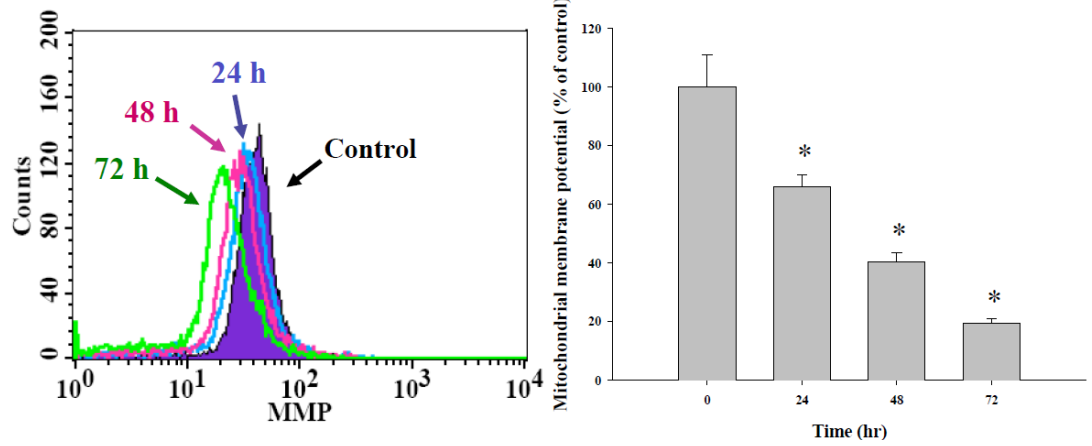
Counts
MMP
Control
24 h
48 h
72 h
Mitochondrial membrane potential (% of control)
Time (hr)

C

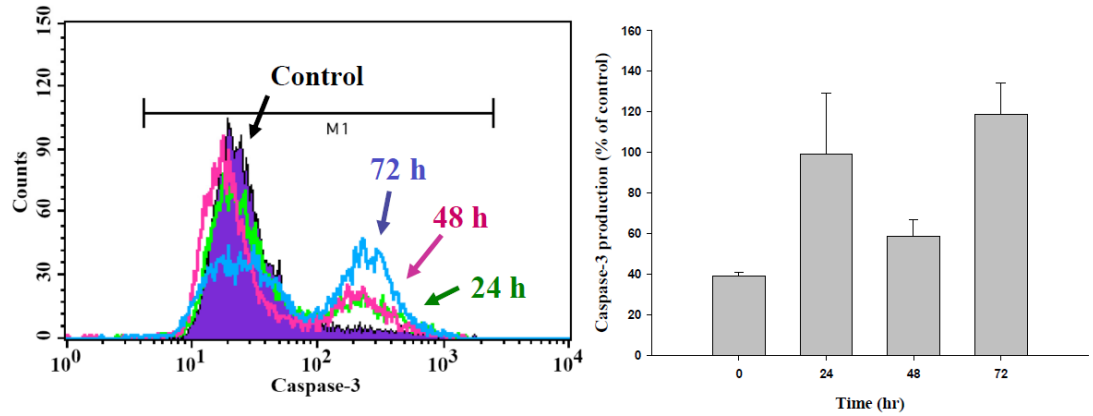
Counts
Caspase-3
Control
M1
72 h
48 h
24 h
Caspase-3 production (% of control)
Time (hr)

Figure 5

A

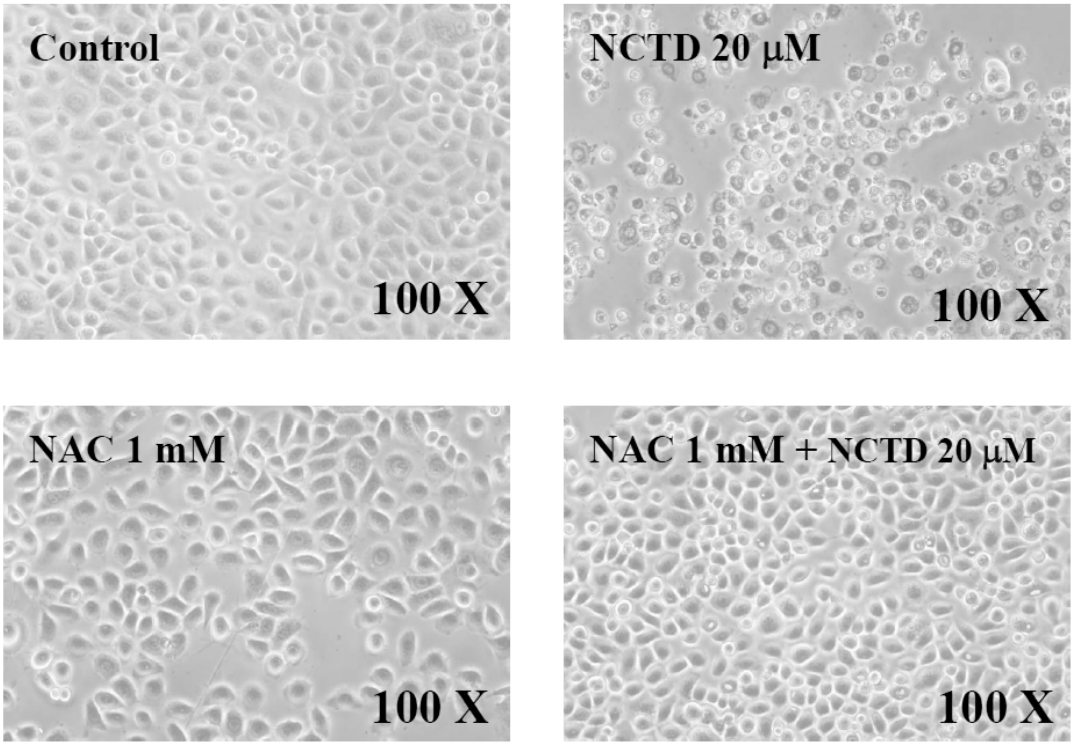
Control
100 X
NCTD 20 μM
100 X
NAC 1 mM
100 X
NAC 1 mM + NCTD 20 μM
100 X

B

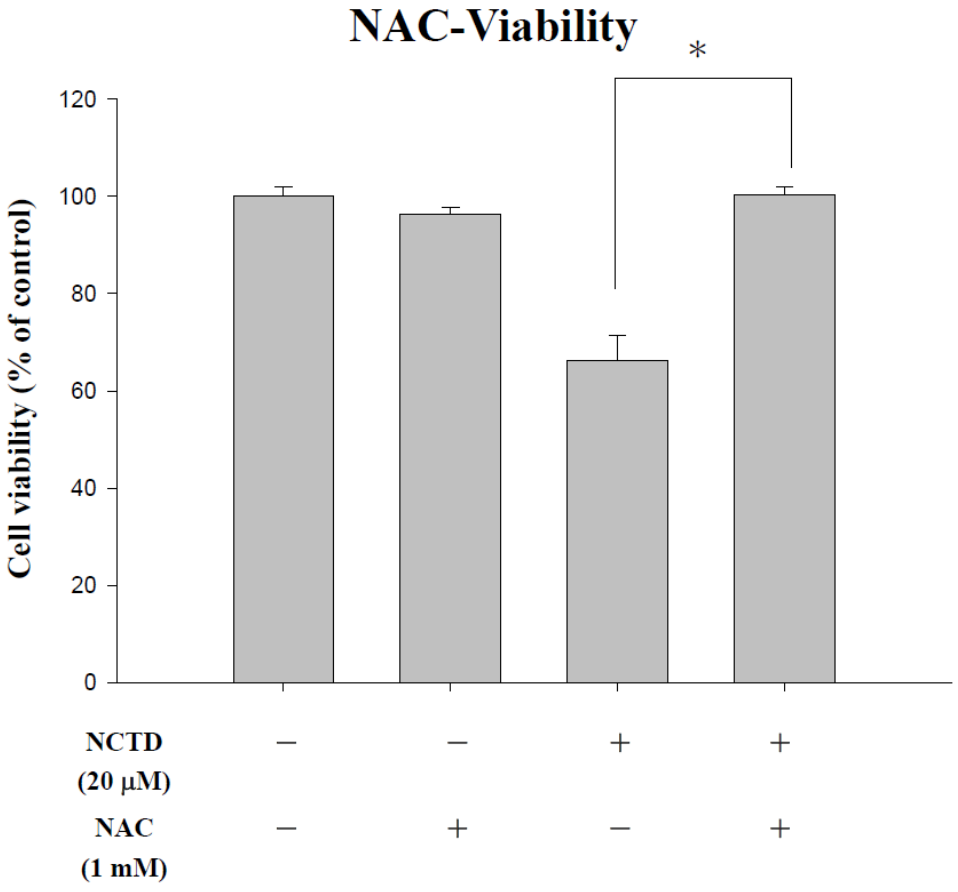
NAC-Viability
*
Cell viability (% of control)
120
100
80
60
40
20
0
NCTD
(20 μM)
NAC
(1 mM)
−
−
+
+
−
+
−
+

C

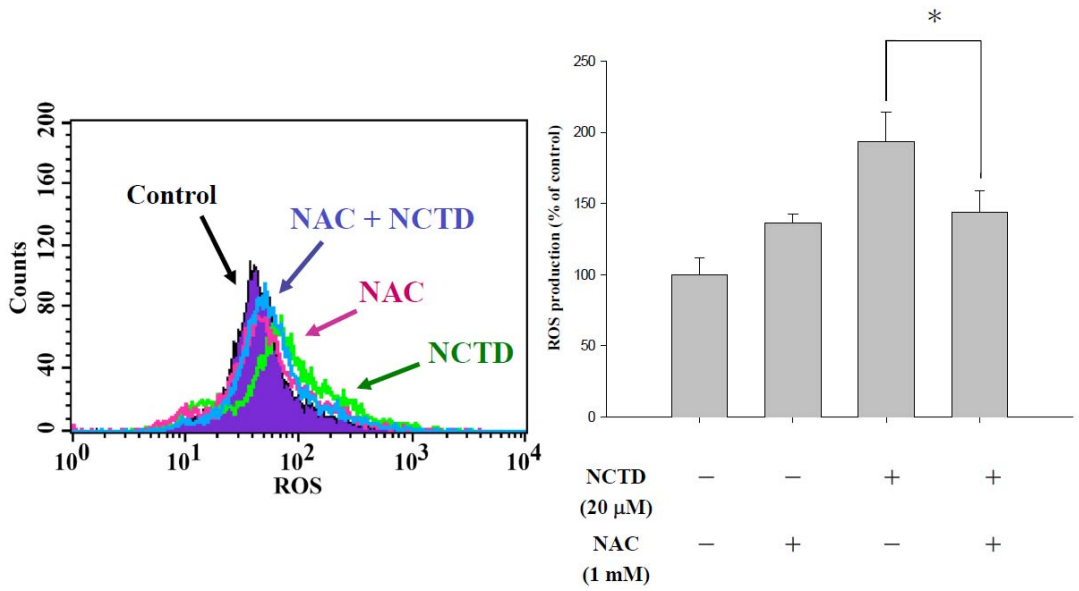
Control
NAC + NCTD
NAC
NCTD
Counts
ROS
ROS production (% of control)
*
NCTD (20 μM)
NAC (1 mM)

D

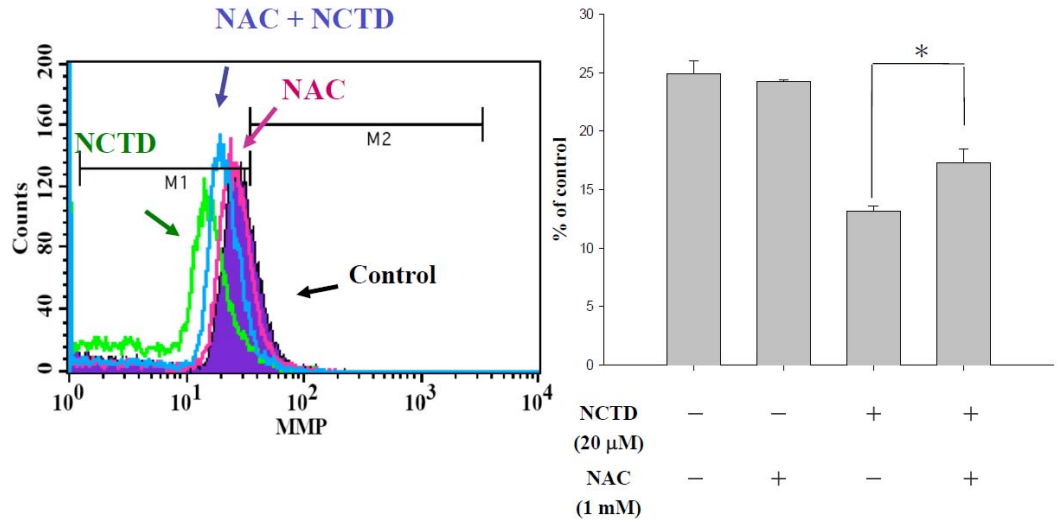
NAC + NCTD
NAC
NCTD
M1
M2
Control
Counts
MMP
% of control
*
NCTD (20 μM)
NAC (1 mM)

E

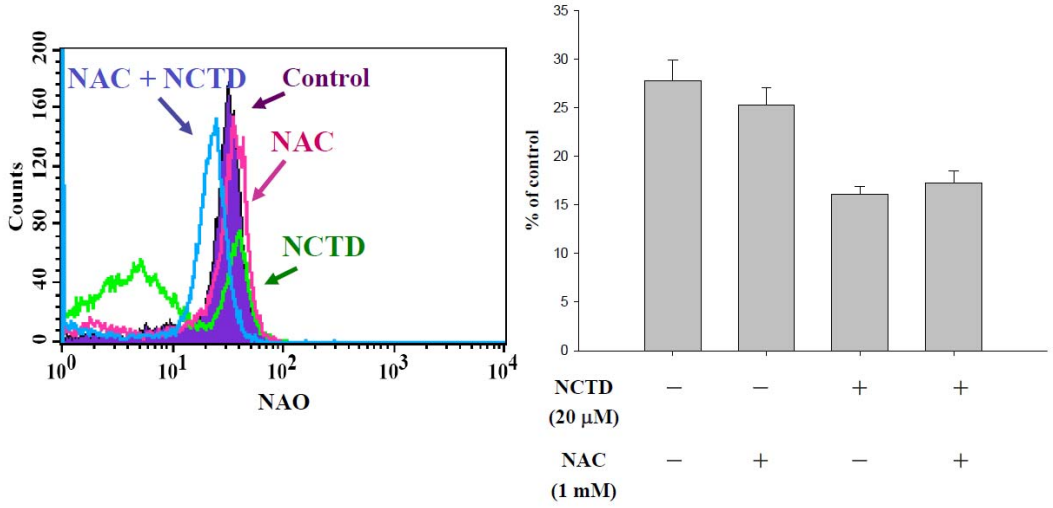
NAC + NCTD
Control
NAC
NCTD
Counts
NAO
% of control
NCTD (20 μM)
NAC (1 mM)

F

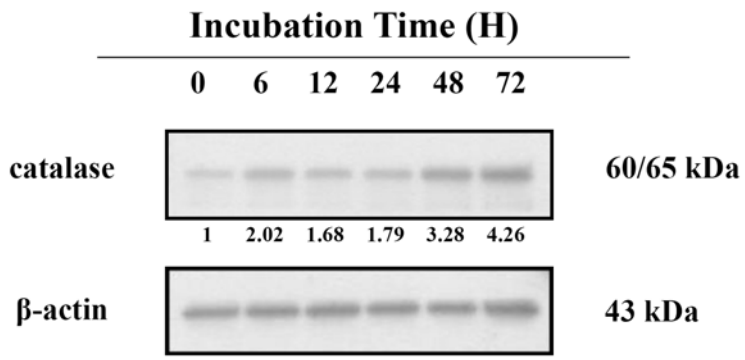
Incubation Time (H)
0 6 12 24 48 72
catalase
60/65 kDa
1 2.02 1.68 1.79 3.28 4.26
β-actin
43 kDa

Figure 6

A

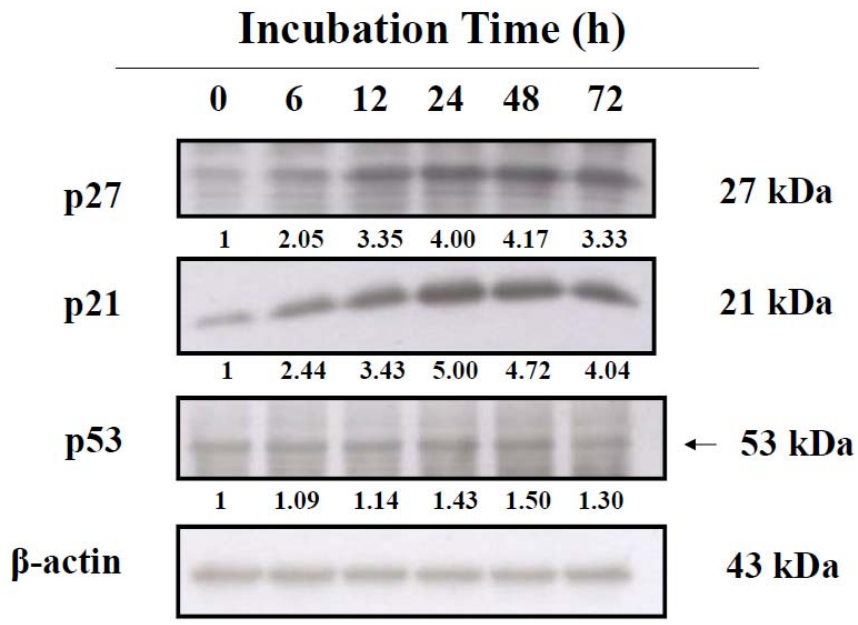
Incubation Time (h)
0 6 12 24 48 72
p27
27 kDa
1 2.05 3.35 4.00 4.17 3.33
p21
21 kDa
1 2.44 3.43 5.00 4.72 4.04
p53
53 kDa
1 1.09 1.14 1.43 1.50 1.30
β-actin
43 kDa

B

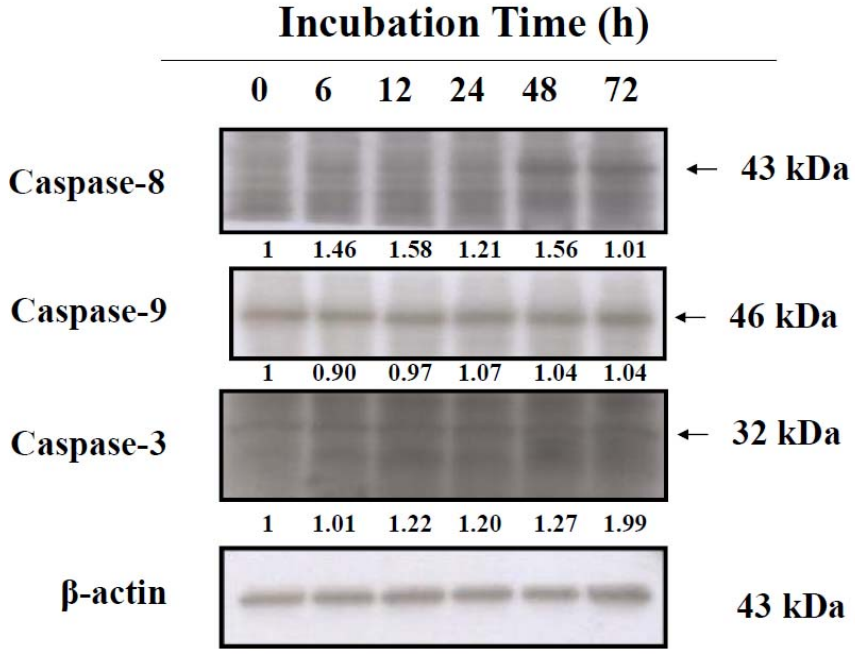
Incubation Time (h)
0 6 12 24 48 72
Caspase-8
43 kDa
1 1.46 1.58 1.21 1.56 1.01
Caspase-9
46 kDa
1 0.90 0.97 1.07 1.04 1.04
Caspase-3
32 kDa
1 1.01 1.22 1.20 1.27 1.99
β-actin
43 kDa

C

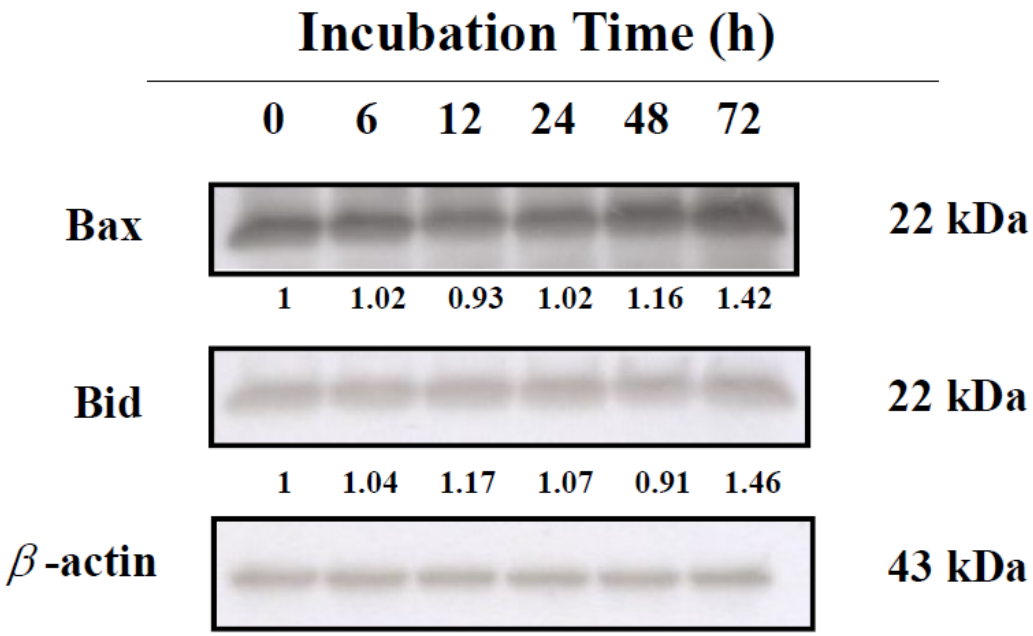
Incubation Time (h)
0 6 12 24 48 72
Bax
22 kDa
1 1.02 0.93 1.02 1.16 1.42
Bid
22 kDa
1 1.04 1.17 1.07 0.91 1.46
β-actin
43 kDa

D

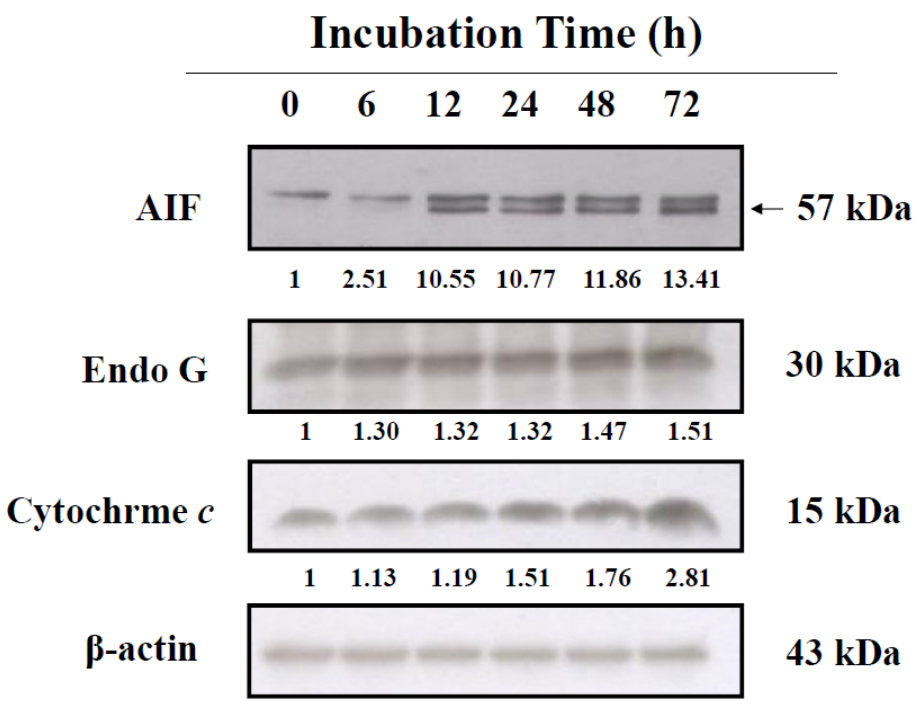
Incubation Time (h)
0 6 12 24 48 72
AIF
← 57 kDa
1 2.51 10.55 10.77 11.86 13.41
Endo G
30 kDa
1 1.30 1.32 1.32 1.47 1.51
Cytochrme c
15 kDa
1 1.13 1.19 1.51 1.76 2.81
β-actin
43 kDa

E

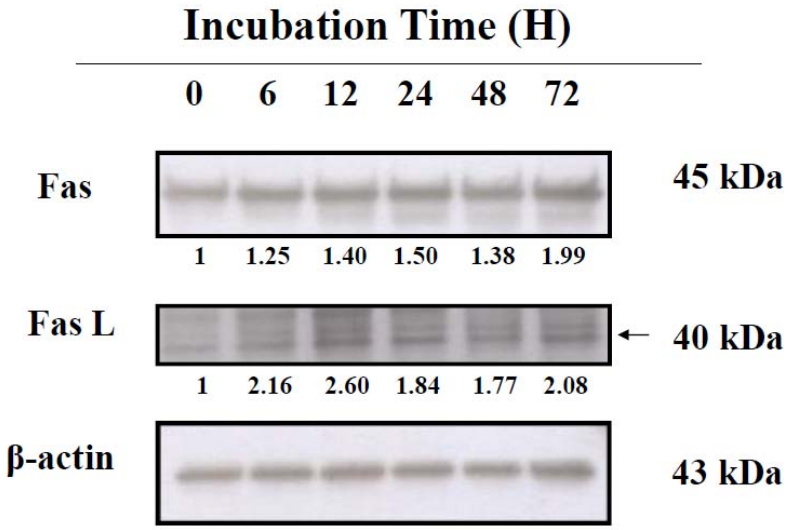
Incubation Time (H)
0 6 12 24 48 72
Fas
45 kDa
1 1.25 1.40 1.50 1.38 1.99
Fas L
40 kDa
1 2.16 2.60 1.84 1.77 2.08
β-actin
43 kDa

F

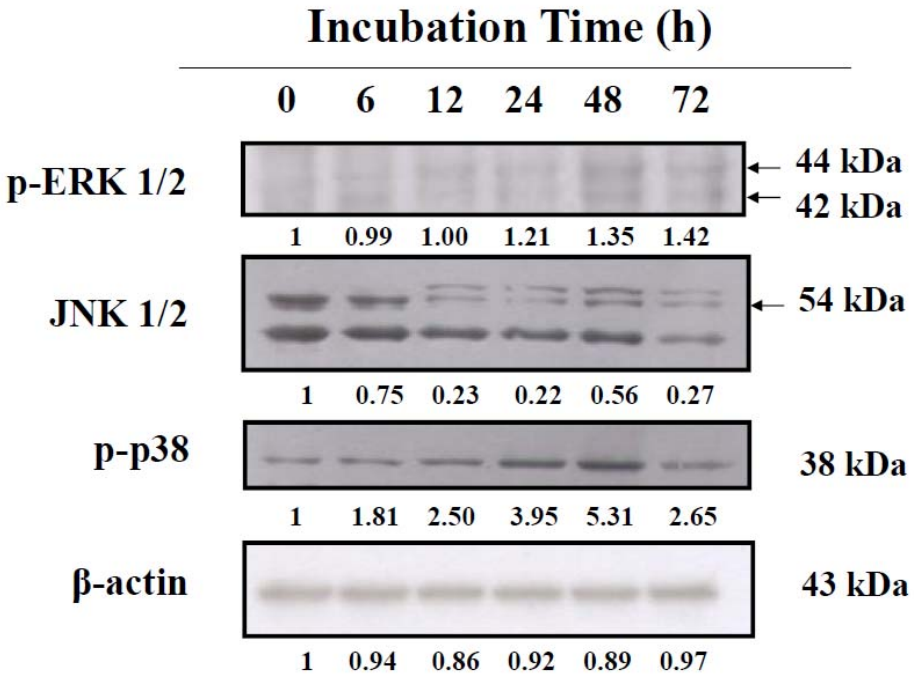
Incubation Time (h)
0 6 12 24 48 72
p-ERK 1/2
44 kDa
42 kDa
1 0.99 1.00 1.21 1.35 1.42
JNK 1/2
54 kDa
1 0.75 0.23 0.22 0.56 0.27
p-p38
38 kDa
1 1.81 2.50 3.95 5.31 2.65
β-actin
43 kDa
1 0.94 0.86 0.92 0.89 0.97

Figure 7

A

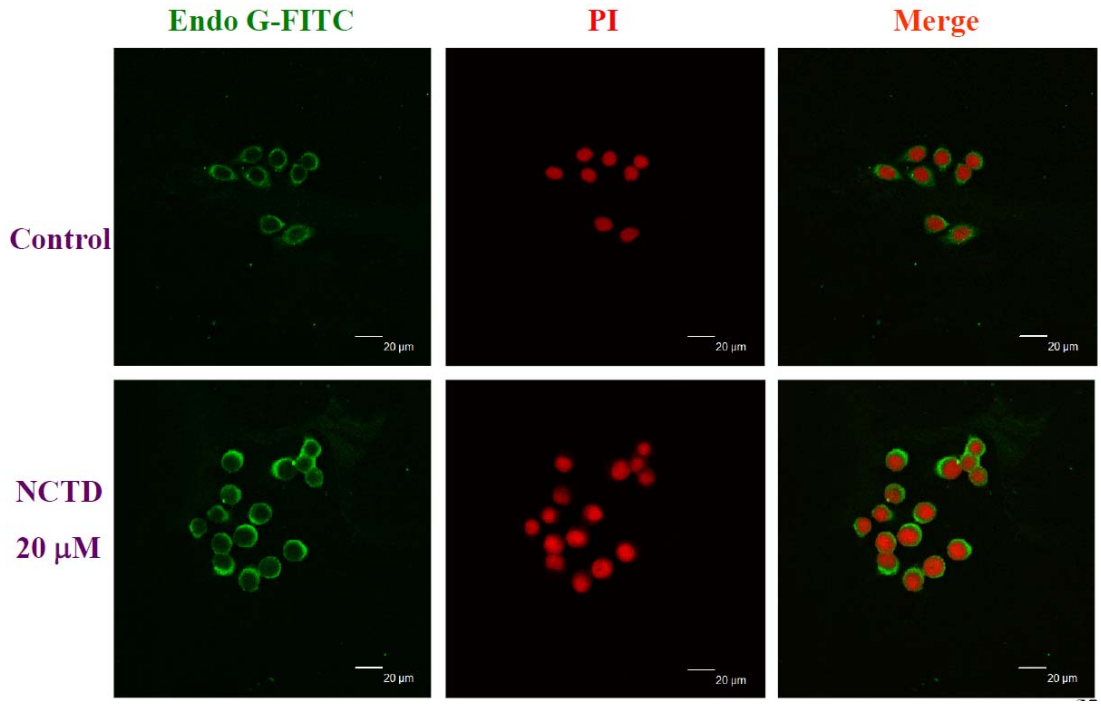
Endo G-FITC
PI
Merge
Control
NCTD
20 μM
20 μm

B

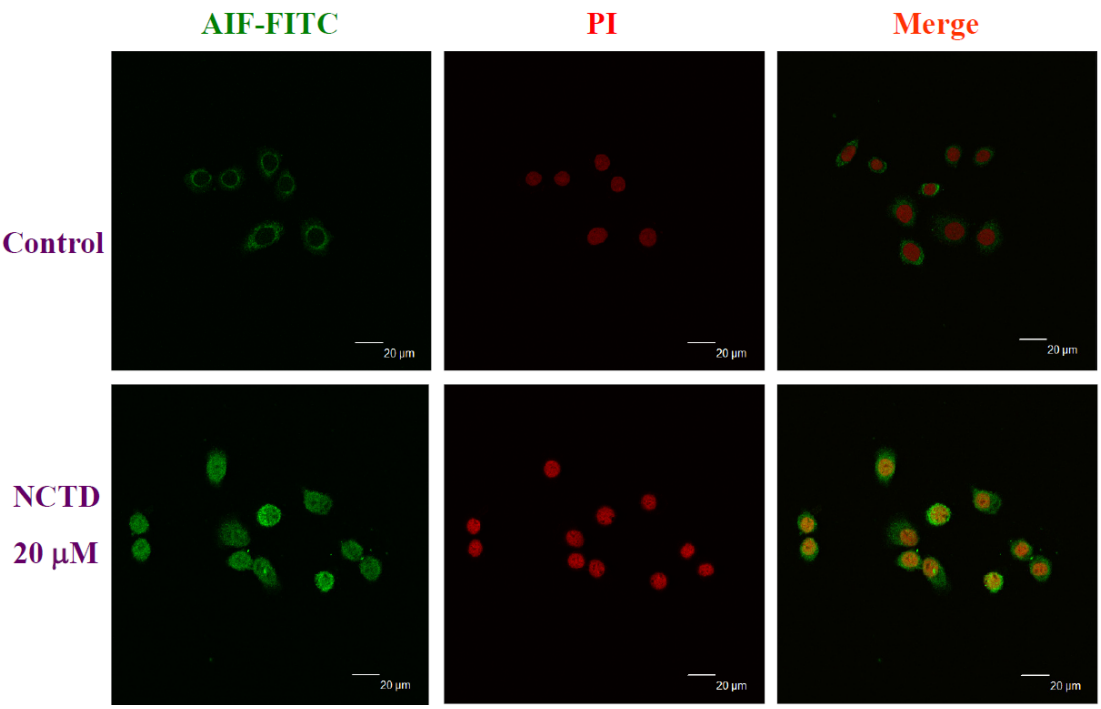
AIF-FITC
PI
Merge
Control
NCTD
20 μM
20 μm

Figure 8

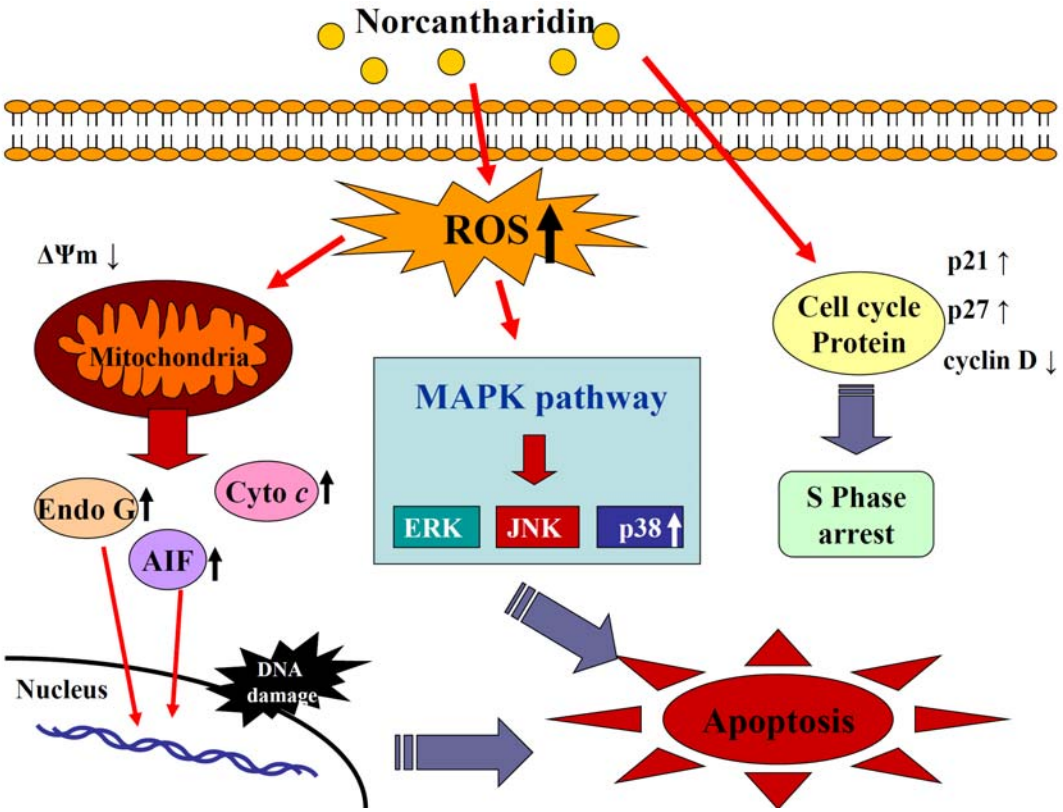
Norcantharidin
ROS
ΔΨm ↓
Mitochondria
Endo G
Cyto c
AIF
Nucleus
DNA damage
MAPK pathway
ERK
JNK
p38
Cell cycle Protein
p21 ↑
p27 ↑
cyclin D ↓
S Phase arrest
Apoptosis